Molecular opacities of low-lying states of oxygen molecule*

Gui-Ying Liang(梁桂颖)[1], Yi-Geng Peng(彭裔耕)[1,†], Rui Li(李瑞)[1,3], Yong Wu(吴勇)[1,2,‡], and Jian-Guo Wang(王建国)[1]

[1] *Institute of Applied Physics and Computational Mathematics, Beijing* 100088, *China*
[2] *HEDPS, Center for Applied Physics and Technology, Peking University, Beijing* 100084, *China*
[3] *Department of Physics, College of Science, Qiqihar University, Qiqihar* 161006, *China*

(Received 23 October 2019; revised manuscript received 2 December 2019; accepted manuscript online 9 December 2019)

The $X^3\Sigma_g^-$, $A'^3\Delta_u$, $A^3\Sigma_u^+$, $1^3\Pi_g$, and $B^3\Sigma_u^-$ electronic states of oxygen molecule (O_2) are calculated by the multi-configuration self-consisted filed (MRCI) + Q method with the scalar relativistic correction and core–valence correlation correction. The obtained spectroscopic constants of the low-lying bound states are in excellent agreement with measurements. Based on the accurately calculated structure parameters, the opacities of the oxygen molecule at the temperatures of 1000 K, 2000 K, 2500 K, and 5000 K under a pressure of 100 atm (1 atm = 1.01325×10^5 Pa) and the partition functions between 10 K and 10^4 K are obtained. It is found that with the increase of temperature, the opacities for transitions in a long wavelength range are enlarged because of the larger population on excited electronic states at the higher temperatures.

Keywords: oxygen molecule, transition dipole moments, opacities

PACS: 31.50.Df, 31.15.ag, 31.15.aj **DOI:** 10.1088/1674-1056/ab5fb6

1. Introduction

The oxygen molecule (O_2), which plays an important role in the photo-physical, photochemical, and atmospheric spectroscopy, has received considerable attention over several decades.[1–7] The accurate and detailed information about the electronic states of O_2, *i.e.*, $X^3\Sigma_g^-$ state and low-lying excited states, the potential energy curves (PECs), and transition properties, which are significant for knowing more about spectrum of many kinds of molecules,[8–10] are required to understand the mechanism of the chemical reactions including oxygen molecule[11–17] and to evaluate the abundance of oxygen element in the universe and atmosphere.[15,18,19]

The experimental investigations were performed for the ground state and several low-lying electronic states[20–22] several decades ago. The Raman spectra of O_2 and its isotopic molecules were observed in 1976, and some of the rotational constants for the ground state were analyzed.[23] The vibrational energy levels and spectroscopic parameters of the $A^3\Sigma_u^+$ state were acquired from high-resolution spectrum of the $A^3\Sigma_u^+$–$X^3\Sigma_g^-$ system by Borrell *et al.* in 1986.[24] The absorption bands of the $A^3\Sigma_u^+$–$X^3\Sigma_g^-$ system were measured with a resolution of 0.06 cm^{-1} by Yoshino *et al.*, who presented the vibrational energy levels for the $A^3\Sigma_u^+$ electronic state.[25] Then, the excitation spectrum of the $A^3\Sigma_u^+$ and $A'^3\Delta_u$ states were recorded by exciting the higher states with dye-laser emission at the $\lambda = 249$ nm by Wildt *et al.*[26] In 1999, Jenouvrier *et al.*[27] re-investigated the absorption spectra of Herzberg band systems ($A^3\Sigma_u^+$–$X^3\Sigma_g^-$ and $A'^3\Delta_u$–$X^3\Sigma_g^-$). The positions of the lines were analyzed and more accurate energy levels were obtained for the $A'^3\Delta_u$ and $A^3\Sigma_u^+$ states. The spectra of Herzberg II system located in the near-infrared nightglow region and visible region for O_2 were observed by Muñoz *et al.*,[28] who provided more information about the spectrum of O_2 and extended the range of the spectrum. The vibrational energy levels of $v = 11$–18 for the $X^3\Sigma_g^-$ were re-investigated in the flash photolysis studies in absorption spectrum of $B^3\Sigma_u^-$–$X^3\Sigma_g^-$ band at the Doppler-limited resolution which provided more accurate experimental data.[29] The spectroscopic constants of O_2 were obtained by analyzing the corresponding spectrum. The emission spectrum of transition from $B^3\Sigma_u^-$ to the $X^3\Sigma_g^-$ in a wavelength range of 2116 Å −5663 Å was measured by Ekt *et al.*[30]

A series of theoretical work was also carried out for O_2. Dating back to 1968, the 62 low-lying electronic states were calculated by Schaefer *et al.*[31] The spectroscopic constants of O_2, including several low-lying states, were presented by a battery of theoretical computations.[32–40] Then the transitions between triplet states were calculated by the multi-configuration self-consisted filed (MCSCF) method,[41,42] which can be used to learn more about the radiative information of O_2. And Minaev *et al.*[43] evaluated the transition dipole moments between valence states. The accurate spectroscopic constants for the ground and excited electronic states, including $X^3\Sigma_g^-$, $A'^3\Delta_u$, $A^3\Sigma_u^+$, $B^3\Sigma_u^-$, and $1^3\Pi_g$ states, were determined in recent years.[44,45]

As mentioned above, extensive studies of O_2 both experimentally and theoretically have been carried out: most of those

*Project supported by the National Key Research and Development Program of China (Grant No. 2017YFA0402300), the National Natural Science Foundation of China (Grant Nos. 11934004, 11404180, and 11604052), and the China Postdoctoral Science Foundation (Grant No. 2018M631404).

†Corresponding author. E-mail: pygdmn@mail.ustc.edu.cn
‡Corresponding author. E-mail: wu_yong@iapcm.ac.cn

studies mainly concentrated on electronic structure and spectroscopic constant calculations. In addition, systematic studies of the radiative properties, which are very important for explaining spectroscopic diagnosis in the atmosphere, are still lacking. In this work, the accurate PECs and transition dipole moments are calculated with high-level *ab initio* method. The scalar relativistic effect is concerned and the core–valence (CV) correlation effect, which is always neglected, is carefully evaluated. Then the opacities and partition functions are presented at different temperatures under a pressure of 100 atm.

2. Theoretical method

The electronic structure is calulated with the Molpro 2010 program package.[46] The aug-cc-pwCV5Z-DK Gaussian basis,[47] which can describe the CV effect and relativistic effect better, is located on each O atom. The internuclear distance varies from 0.975 Å to 6.0 Å. The reduced D_{2h} group is employed to replace the $D_{\infty h}$ point group which is not suitable for practical quantum chemistry use. The relationships between irreducible representations of $D_{\infty h}$ and D_{2h} are $\Sigma_g^+ \to A_g$, $\Sigma_u^+ \to B_{1u}$, $\Sigma_g^- \to B_{1g}$, $\Sigma_u^- \to A_u$, $\Pi_g \to B_{2g} + B_{3g}$, and $\Pi_u \to B_{2u} + B_{3u}$. Starting from the HF MOs of the ground state, the state-averaged complete active space self-consistent filed (SA-CASSCF) method is employed to construct the multi-configuration wavefunction which can include the degeneracy and near-degeneracy of all the computed states. Then, the internally contracted multi-reference configuration interaction (icMRCI) method, which can deal with the dynamical electron correlation, is used to calculate the PEC as well as the transition dipole moment. In the above SA-CASSCF calculation, ten outermost molecular orbitals (MOs) (two A_g, two B_{3u}, two B_{2u}, two B_{1u}, one B_{2g}, and one B_{3g}), which correspond to the 2s2p shell of the O atom and an additional π_u orbital as found necessary for the appropriate description of the transition probabilities, are involved in the active space. The Davidson correction (+Q) is taken into consideration to correct the size-consistency error of the icMRCI method. In order to obtain the accurate PECs, the third-order Douglas–Kroll–Hess one-electron integrals are used to consider the scalar relativistic effect. In order to evaluate the effect of the CV correlation, which is also important for the high-level quantum chemical calculations, the calculations are carried out by including and excluding the CV correlation. When the CV correction is excluded, the core shell 1s electrons of O are kept closed in the MRCI calculation. When the CV correction is included, all the electrons are correlated in the MRCI calculation. Based on the PECs, the spectroscopic constants, including harmonic vibrational frequency (ω_e), anharmonic constant ($\omega_e x_e$), adiabatic transition energy (T_e), rotational constant (B_e), and equilibrium bond length (R_e), for the concerned bound states are obtained by the numerical method from the LEVEL program.[48]

Under the well-known Born–Oppenheimer approximation, the motion of nuclei and electrons can be separated from each other. Hence, the Hamiltonian can be expressed as

$$\hat{H} = \hat{H}_e + \hat{T}_N, \tag{1}$$

where $\hat{H}_e$ is the Hamiltonian of the electron which can be replaced by the potential energy, and $\hat{T}_N$ represents the kinetic energy term of nucleus.

The nucleus movement is represented by the ro-vibrational states which can be obtained by solving the radical nuclear Schrödinger equation, as follows:

$$\left[-\frac{1}{2\mu}\frac{\mathrm{d}^2}{\mathrm{d}R^2} + E_n(R) + \frac{J(J+1)}{2\mu R^2}\right]\chi_{n\upsilon J}(R) = E_{n\upsilon J}\chi_{n\upsilon J}(R), \tag{2}$$

where $E_{n\upsilon J}$ is the ro-vibrational energy level for the electronic state n, and $E_n(R)$ is the potential energy of the electronic state.

The Einstein coefficient, which reflects the rate for the radiative process between two levels, is described by

$$A_{n'\upsilon'J',n''\upsilon''J''} = \frac{4}{3}\alpha^3\omega^3_{n'\upsilon'J',n''\upsilon''J''}\frac{S_{J'J''}}{2J''+1}, \tag{3}$$

where α is the fine-structure constant, $\omega_{n'\upsilon'J',n''\upsilon''J''}$ is the transition frequency between two ro-vibrational levels, and the line strength $S_{J'J''}$ is determined by

$$S_{J'J''} = \left|\langle\chi_{n'\upsilon'J'}\left|D_{n'n''}(R)\right|\chi_{n''\upsilon''J''}\rangle\right|^2\phi_{J'J''}. \tag{4}$$

The transition dipole moment function $D(R)$ between n' and n'' electronic state can be defined as

$$D_{n'n''}(R) = \int \Psi_{n'}(r,R)\sum_i e\boldsymbol{r}_i\Psi_{n''}(r,R)\,\mathrm{d}\boldsymbol{r}, \tag{5}$$

and $\Psi_{n'}(r,R)$ and $\Psi_{n''}(r,R)$ are the wavefunctions of upper state and lower state, respectively. The Hönl–London factor $\phi_{J'J''}$ is

$$\phi_{J',J''} = \begin{cases} \Delta\Lambda = 0, \dfrac{(J''+\Lambda'')(J''-\Lambda'')}{J''}, \\ \Delta\Lambda = +1, \dfrac{(J''-1-\Lambda'')(J''-\Lambda'')}{4J''}, \\ \Delta\Lambda = -1, \dfrac{(J''-1+\Lambda'')(J''+\Lambda'')}{4J''}, \end{cases} (\mathrm{P-branch}),$$

$$\phi_{J',J''} = \begin{cases} \Delta\Lambda = 0, \dfrac{(2J''+1)\Lambda''^2}{J''(J''+1)}, \\ \Delta\Lambda = +1, \dfrac{(J''+1+\Lambda'')(J''-\Lambda'')(2J''+1)}{4J''(J''+1)}, \\ \Delta\Lambda = -1, \dfrac{(J''+1-\Lambda'')(J''+\Lambda'')(2J''+1)}{4J''(J''+1)}, \end{cases} (\mathrm{Q-branch}),$$

$$\phi_{J',J''} = \begin{cases} \Delta\Lambda = 0, \dfrac{(J''+1+\Lambda'')(J''+1-\Lambda'')}{J''+1}, \\ \Delta\Lambda = +1, \dfrac{(J''+2+\Lambda'')(J''+1+\Lambda'')}{4(J''+1)}, \\ \Delta\Lambda = -1, \dfrac{(J''+2-\Lambda'')(J''+1-\Lambda'')}{4(J''+1)}. \end{cases} (\mathrm{R-branch}). \tag{6}$$

The total internal partition function $Q(T)$ is summed over all the concerned electronic state weighed by the Boltzmann factor utilizing

$$Q = \sum_{i=1}^{n} Q_{ei} Q_{vi} Q_{ri} \exp\left(-\frac{T_i hc}{kT}\right). \tag{7}$$

T_i is the excitation energy of electronic state i, and T is the temperature of the environment.

Molecular opacity, which can describe the radiative property of the atom or molecule, can be obtained with the spectrum parameters to be

$$\sigma = \frac{1}{8\pi(E''/hc)^2} \times \frac{A(2J'+1)\exp(-E''hc/kT)[1-\exp(-\Delta E_{V'J',00}/kT]}{Q}, \tag{8}$$

where $\Delta E_{V'J',00}$ is the ro-vibrational excitation energy relative to ground state, and E'' is the energy gap between the concerned two states.

3. Results and discussion

3.1. PECs and spectroscopic constants

With the method mentioned above, the PECs of the five low-lying electronic states, *i.e.*, $X^3\Sigma_g^-$, $A^3\Sigma_u^+$, $1^3\Pi_g$, $A'^3\Delta_u$, and $B^3\Sigma_u^-$, are obtained. For a clear understanding of the CV correlation effect, the PECs are computed with and without considering the CV correlation. The PECs with considering CV correlation are depicted in Fig. 1, but the ones without CV correction are not presented here because their difference from those with considering CV correlation is unrecognizable. As shown in Fig. 1, the $1^3\Pi_g$ is weakly bounded state, and the $X^3\Sigma_g^-$, $A'^3\Delta_u$, $A^3\Sigma_u^+$, and $B^3\Sigma_u^-$ are all typical bound states. The $X^3\Sigma_g^-$, $A'^3\Delta_u$, $A^3\Sigma_u^+$, and $1^3\Pi_g$ states correspond to the lowest $O(^3P)+O(^3P)$ asymptotic limit, and the $B^3\Sigma_u^-$ state is correlated to the $O(^3P)+O(^1D)$ asymptotic limit. The PEC of $1^3\Pi_g$ state has a small shoulder around the internuclear spacing of 1.75 Å, which comes from the avoided crossing caused by higher electronic states. The energy gap between the asymptotic limits is 15805.158 cm^{-1} which is only 62.704 cm^{-1} deviation from the experimental excitation energy between $O(^3P)$ and $O(^1D)$ of 15867.862 cm^{-1}.[49]

On the basis of the calculated PECs, the spectroscopic constants derived from the CV concerned and CV excluded PECs are presented in Table 1 together with the available experimental and theoretical data. The CV concerned spectroscopic constants for all the five states $X^3\Sigma_g^-$, $A'^3\Delta_u$, $A^3\Sigma_u^+$, $B^3\Sigma_u^-$, and $1^3\Pi_g$ are in better agreement with the experimental values[20–22] than the CV excluded ones, *e.g.*, the ω_e, $\omega_e x_e$, B_e, and R_e of the ground state $X^3\Sigma_g^-$ excluding CV correction, which specifically are 1568.5599 cm^{-1}, 11.3589 cm^{-1}, 1.4386 cm^{-1}, and 1.2105 cm^{-1}, respectively. The deviations 11.6301 cm^{-1}, 0.6211 cm^{-1}, 0.00703 cm^{-1}, and 0.00298 Å relative to the measured values, are larger than those including the CV correction, *i.e.*, 5.06 cm^{-1}, 0.5614 cm^{-1}, 0.00183 cm^{-1}, and 0.00078 Å.

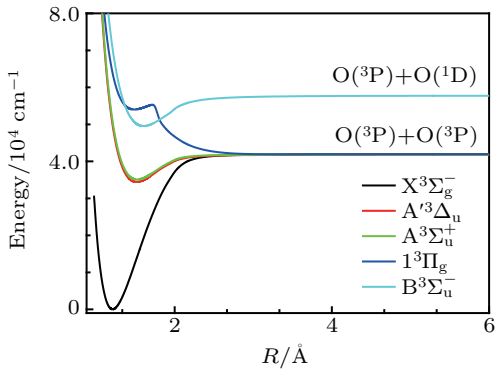

Fig. 1. MRCI $+Q$ PECs of O_2 for $X^3\Sigma_g^-$, $A^3\Sigma_u^+$, $1^3\Pi_g$, $A'^3\Delta_u$, and $B^3\Sigma_u^-$ states with CV correction.

The most recent calculations of Minaev *et al.*,[42] Müller *et al.*,[44] and Jiang *et al.*[45] have comparable precision to the present results. So here we mainly compare the present spectroscopic constants with the values of Minaev *et al.*,[42] Müller *et al.*,[44] Jiang *et al.*,[45] and experiments[20–22] for each state. For the ground state $X^3\Sigma_g^-$, the dominant electronic configuration is $2\sigma_g^2 2\sigma_u^2 3\sigma_g^2 1\pi_u^4 1\pi_g^2$ (93.43%) at equilibrium bond length. The present spectroscopic constants are better agreement on the whole with experiment[20] than those from other theories except the results presented by Minaev *et al.*[42] The first excited state $A'^3\Delta_u$ is characterized mainly by $2\sigma_g^2 2\sigma_u^2 3\sigma_g^2 1\pi_u^3 1\pi_g^3$ (92.85%) configuration arising from the $1\pi u \rightarrow 1\pi_g$ excitation from the ground state $X^3\Sigma_g^-$. The present R_e value, which is more accurate than any other previous calculated values,[31,33,37–41,43–45] is in excellent agreement with experimental data.[21] Other spectroscopic constants of Müller *et al.*[44] are in better agreement with experimental data.[21] For $A^3\Sigma_u^+$ state with the main electronic configuration of $2\sigma_g^2 2\sigma_u^2 3\sigma_g^2 1\pi_u^3 1\pi_g^3$ (92.32%), its ω_e and T_e presented by Müller *et al.*[44] are in better agreement with measurements. The $B^3\Sigma_u^-$ state corresponds to a mixed configuration of $2\sigma_g^2 2\sigma_u^2 3\sigma_g^2 1\pi_u^3 1\pi_g^3$ (68.60%) and $2\sigma_g^2 2\sigma_u^2 3\sigma_g^1 3\sigma_u^1 1\pi_u^4 1\pi_g^2$ (27.77%). The present R_e value is in better agreement with the experimental values than those given by Minaev *et al.*[42] Müller *et al.*[44] and Jiang *et al.*[45] The $1^3\Pi_g$ state has the leading electronic configuration of $2\sigma_g^2 2\sigma_u^2 3\sigma_g^1 1\pi_u^4 1\pi_g^3$ (90.95%) at equilibrium bond length. And the main electronic configurations change from $2\sigma_g^2 2\sigma_u^2 3\sigma_g^2 3\sigma_u^1 1\pi_u^3 1\pi_g^2$ (85.18%) near $R \sim 1.75$ Å to diffused configuration combination of $2\sigma_g^2 2\sigma_u^2 3\sigma_g^2 3\sigma_u^1 1\pi_u^3 1\pi_g^2$ (62.33%)+$2\sigma_g^2 2\sigma_u^2 3\sigma_g^2 3\sigma_u^1 1\pi_u^1 1\pi_g^4$ (7.09%)+$2\sigma_g^2 2\sigma_u^2 3\sigma_g^1 3\sigma_u^2 1\pi_u^2 1\pi_g^3$ (11.68%) at $R > 1.75$ Å. The present results are in good agreement with the values obtained by Mü ller *et al.*[44] and Jiang *et al.*[45] but no reliable experimental values are reported.

Table 1. Computed and measured spectroscopic constants for low-lying electronic states of O_2.

State	Method	T_e/cm^{-1}	ω_e/cm^{-1}	$\omega_e\chi_e$/cm^{-1}	B_e/cm^{-1}	R_e/cm^{-1}
$X^3\Sigma_g^-$	Present[a]	0	1568.5599	11.3589	1.4386	1.2105
	Present[b]	0	1575.1300	11.4186	1.4438	1.2083
	Expt.[c]	0	1580.19	11.98	1.44563	1.2075
	CI[f]	0	1582	14	1.25	1.30
	Full valence CI[g]	0	1673			1.278
	CI[h]	0	1498.8	9.87	1.38	1.236
	MRCI + Q[i]	0	1549	11.54	1.4188	1.219
	MCSCF[j]	0	1525.9	16.97	1.42	1.219
	MRSDCI[j]		1538.7	16.75	1.42	1.217
	MRSDCI + Q[j]		1522.9	17.02	1.41	1.221
	VBSCF[k]		1550			1.206
	MCSCF[l]	0	1577.6			1.211
	MRCISD + Q[m]	0	1593			1.2105
	icMRCI + Q[n]		1557.6			1.2162
$A'^3\Delta_u$	Present[a]	34418.592	865.8228	21.9202	0.9182	1.5150
	Present[b]	34658.488	865.2053	21.7057	0.9213	1.5129
	Expt.[d]	34770	815			1.5129
	CI[f]		958	27	0.88	1.550
	Full valence CI[g]	34762.482	990			
	CI[h]	33310.684	780	13.18	0.877	1.550
	MCSCF[l]	34565.06	842			1.516
	MRCISD + Q[m]	34721	813			1.5148
	icMRCI + Q[n]	33813	796.3			1.5249
$A^3\Sigma_u^+$	Present[a]	35045.069	869.6288	24.6010	0.9097	1.5225
	Present[b]	35288.372	872.2330	24.7339	0.9128	1.5199
	Expt.[d]	35399.659	799.1	12.16	0.911	1.522
	CI[f]		943	29	0.87	1.56
	Full valence CI[g]	35407.725	977			1.525
	CI[h]	33923.665	764.6	13.94	0.868	1.558
	MCSCF[l]	35500.022	832.8			1.522
	MRCISD + Q[m]	35355	799			1.5219
	icMRCI + Q[n]	34438	781.0			1.5322
$B^3\Sigma_u^-$	Present[a]	49537.123	761.6070	13.8285	0.8180	1.6055
	Present[b]	49918.510	768.4142	14.2351	0.8196	1.6038
	Expt.[c]	49793.585	709.31	10.65	0.82	1.6042
	Expt.[e]	48534	728	12.33		
	CI[f]		593	−27	0.74	1.68
	Full valence CI[g]	51135.529	697			1.648
	CI[h]	49030.424	724.9	7.04	0.791	1.627
	MCSCF[l]	52098.888	733.6			1.596
	MRCISD + Q[m]	49338	722			1.5998
	icMRCI + Q[n]	49760	709.7			1.6093
$1^3\Pi_g$	Present[a]	54214.583	682.7576	40.0636	0.9628	1.4814
	Present[b]	54010.506	681.3590	42.7632	0.9572	1.4865
	Expt.[c]	65530	1840			
	MRCISD + Q[m]	54108	689			1.4828
	icMRCI + Q[n]	53809	677.6			1.4906

[a]present calculation excluding core–valence; [b]present calculation including core–valence; [c]Ref. [20]; [d]Ref. [21]; [e]Ref. [22]; [f]Ref. [31]; [g]Ref. [40]; [h]Ref. [33]; [i]Ref. [37]; [j]Ref. [38]; [k]Ref. [39]; [l]Ref. [42]; [m]Ref. [44]; [n]Ref. [45].

From the comparison above, our results for the ground state $X^3\Sigma_g^-$ are in better agreement with measurements than Müller *et al.*,[44] and the measurements are also performed at the MRCI $+Q$ level to treat the dynamical correlation with valence orbitals derived from 2s and 2p atomic orbitals while the CV correlation is not included. Several spectroscopic constants (*e.g.*, ω_e of the $X^3\Sigma_g^-$) given by Minaev *et al.*[42] are slightly closer to the experimental values. However, in their

calculation, much smaller basis set (aug-cc-pVDZ) and active space (two σ_g, two π_u, two σ_u, and one π_g) were used. The electronic correlation is treated only at the MCSCF level without dynamical correlation or CV effect,[42] so this may be an accidental match. The spectroscopic constants of $B^3\Sigma_u^-$ state calculated by Jiang *et al.*[45] are in better agreement with measurements, but the active space (corresponding to two σ_g, one π_u, two σ_u, and one π_g) used in their calculation is not sufficient and their spectroscopic constants for the ground state $X^3\Sigma_g^-$ and other excited states have lager differences from the measurements than the present ones. So we can infer that the CV correlation effect should be important for the $X^3\Sigma_g^-$ and $B^3\Sigma_u^-$ state. As shown in Subsection 3.3, the $B^3\Sigma_u^-$–$X^3\Sigma_g^-$ transition presents the dominant contribution to the opacities at lower temperature.

3.2. Electronic transition dipole moments

The transition dipole moments among all the calculated states, which are functions of internuclear distance in a range of 0.975 Å-6 Å, are investigated with the MRCI wavefunctions and are depicted in Fig. 2. From Fig. 2 it may follow that the involved transition dipole moments have larger values at small internuclear distances and decrease with the internuclear distance increasing. At large internuclear distances($R > 3.0$ Å), the transition dipole moments tend to zero because the O_2 molecule disintegrate into two neutral atoms mentioned above. Also, the transition dipole moments from $A^3\Sigma_u^+$, $A'^3\Delta_u$, and $B^3\Sigma_u^-$ states to $1^3\Pi_g$ state all have abrupt changes around the internuclear distance of 1.75 Å, which originates from the avoided crossing point of the $1^3\Pi_g$ state. The transition dipole moments from the $X^3\Sigma_g^-$ to the $B^3\Sigma_u^-$ state have lager values than other transitions, which can make stronger contribution to the total cross section.

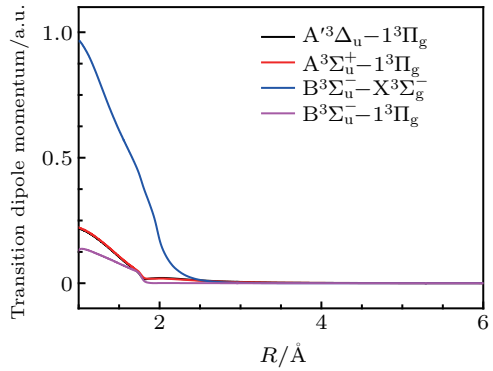

Fig. 2. Spin-allowed transition dipole moments for transitions of $B^3\Sigma_u^-$–$X^3\Sigma_g^-$, $A^3\Sigma_u^+$–$1^3\Pi_g$, $A'^3\Delta_u$–$1^3\Pi_g$, and $B^3\Sigma_u^-$–$1^3\Pi_g$ of O_2 as a function of internuclear distance R.

3.3. Partition function and opacities

With all the ro-vibrational parameters, the partition functions and the opacities of O_2 are determined. Here we calculate the partition function and opacity based on the CV concerned PECs and transition dipole moments. All the results are shown in Figs. 3, 4, and Table 2. The partition function, as a significant parameter for the spectra analysis, relates to the degeneracy, ro-vibrational energy levels and temperature in the local thermodynamic equilibrium (LTE) approximation. As shown in Fig. 3, with the increasing of temperature, the partition function increases gradually, because more excited states are populated.

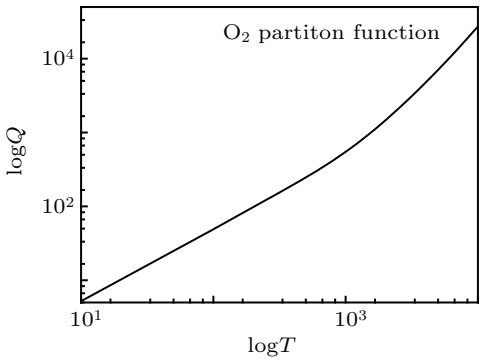

Fig. 3. Partition function for O_2 at temperature ranging from 10 K to 10000 K (T is temperature in Kelvins).

Table 2. Values of partition function Q for O_2 at a series of temperatures (10 K–10000 K) under pressure 100 atm.

T/K	Q	T/K	Q
10	5.189	4000	4740.395
100	48.767	5000	7156.421
200	97.232	6000	10131.131
300	145.812	7000	13689.968
500	245.663	8000	17843.964
1000	545.393	9000	22583.811
2000	1463.668	10000	27879.594
3000	2852.501		

Based on the accurate ro-vibrational energy levels and the transition dipole moments, the opacities of O_2 including the low-lying $X^3\Sigma_g^-$, $A^3\Sigma_u^+$, $1^3\Pi_g$, $A'^3\Delta_u$, and $B^3\Sigma_u^-$ states are obtained with Eq. (8) at temperatures of 1000 K, 2000 K, 2500 K, and 5000 K under a pressure of 100 atm. The simulated spectrum evolves with a Lorentzian line profile[50] according to the collisional broadening with a canonical cross section chosen as 10^{-16} cm^2.[51,52] The cross sections are shown in Figs. 4(a)–4(d). As indicated in Fig. 4(a), at a lower temperature (1000 K), most of molecules are populated on the ground state $X^3\Sigma_g^-$, thus the cross section is located mainly in a shorter wavelength range which predominately comes from the $B^3\Sigma_u^-$-$X^3\Sigma_g^-$ transition. With the increase of temperature, population on excited electronic states $A^3\Sigma_u^+$, $1^3\Pi_g$, $A'^3\Delta_u$, and $B^3\Sigma_u^-$ are enlarged, so the cross sections in a longer wavelength range are enlarged as shown in Figs. 4(b)–4(d). This comes mainly from the transitions between the excited states, *i.e.*, $A^3\Sigma_u^+$–$1^3\Pi_g$, $A'^3\Delta_u$–$1^3\Pi_g$, and $B^3\Sigma_u^-$–$1^3\Pi_g$.

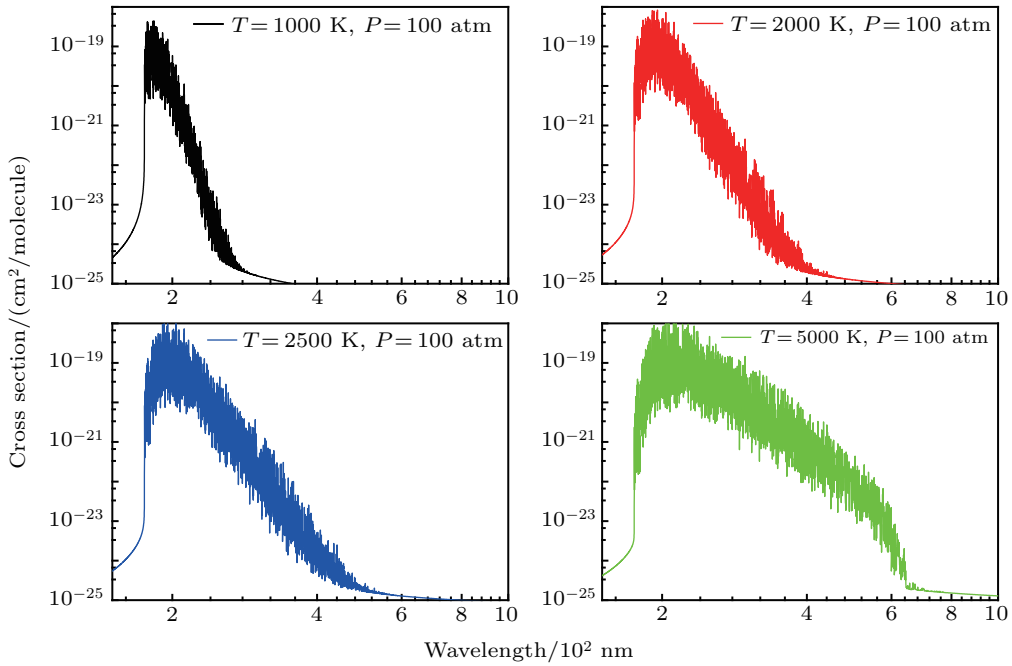

Fig. 4. Opacities of O_2 ro-vibrational transition at temperature of 1000 K, 2000 K, 2500 K, 5000 K under pressure of 100 atm, including transitions of $B^3\Sigma_u^- – X^3\Sigma_g^-$, $A^3\Sigma_u^+ – 1^3\Pi_g$, $A'^3\Delta_u – 1^3\Pi_g$, and $B^3\Sigma_u^- - 1^3\Pi_g$.

4. Conclusions

In present work, accurate PECs and transition dipole moments of the $X^3\Sigma_g^-$, $A^3\Sigma_u^+$, $1^3\Pi_g$, $A'^3\Delta_u$, and $B^3\Sigma_u^-$ states for O_2 are calculated by using the MRCI $+Q$ method, with CV correlation and scalar relativistic effect taken into account. On the basis of the PECs, the corresponding spectroscopic constants, which accord well with the experimental results, are presented. The partition functions including the ro-vibrational levels of these electronic states are presented in a temperature range from 10 K to 10000 K. Based on ro-vibrational wavefunctions derived from the PECs and the transition dipole moments, the absorption cross sections including the considered five electronic states are estimated at the temperatures of 1000 K, 2000 K, 2500 K, and 5000 K under a pressure of 100 atm. It is found that with the increase of the temperature, more excited states are populated. This enlarges the cross section in a long wavelength range. This study will shed light on the radiative properties of oxygen molecule.

Acknowledgement

We thank Dr X Q Hu for helpful discussion.

References

[1] Chamberlain J W 1958 *Astrophys. J.* **128** 713
[2] Geiss J, Gloeckler G, Mall U, von Steiger R, Galvin A B and Ogilvie K W 1994 *Astron. & Astrophys.* **282** 924
[3] Huebner R H, Celotta R J, Mielczarek S R and Kuyatt C E 1975 *J. Chem. Phys.* **63** 241
[4] Trajmar S, Cartwright D C and Hall R I 1976 *J. Chem. Phys.* **65** 5275
[5] Juett A M, Schulz N S and Chakrabarty D 2004 *Astrophys. J.* **612** 1
[6] Du J H and Peng L M 2018 *Chin. Chem. Lett.* **29** 747
[7] Li F, Huang W H and Gong X Q 2018 *Chin. Chem. Lett.* **29** 765
[8] Elkahwagy N, Ismail A, Maize S M A and Mahmoud K R 2018 *Chin. Phys. Lett.* **35** 103101
[9] Wei H L and Liu X J 2018 *Chin. Phys. B* **27** 123101
[10] Cao J J, Gong T, Li Z H, Ji Z H, Zhao Y T, Xiao L T and Jia S T 2018 *Chin. Phys. Lett.* **35** 103301
[11] Hall D T, Strobel D F, Feldman P D, McGrath M A and Weaver H A 1995 *Nature* **373** 677
[12] Meyer D M, Jura M and Cardelli J A 1998 *Astrophys. J.* **493** 222
[13] Aoki W, Norris J E, Ryan S G, Beers T C, Christlieb N, Tsangarides S and Ando H 2004 *Astrophys. J.* **608** 971
[14] Bekker A, Holland H D, Wang P L, Rumble.D I I I, Stein H J, Hannah J L, Coetzee L L and Beukes N J 2004 *Nature* **427** 117
[15] Slanger T G, Pejaković D A, Kostko O, Matsiev D and Kalogerakis K S 2017 *J. Geophys. Res. Space Phys.* **122** 3640
[16] Buldakov M A, Cherepanov V N, Korolev B V and Matrosov I I 2003 *J. Mol. Spectrosc.* **217** 1
[17] Zhang T L, Herbert L, Shi J K, Wang X and Helmut L 2006 *Chin. Phys. Lett.* **23** 2338
[18] Slanger T G, Cosby P C and Huestis D L 2003 *J. Geophys. Res. Space Phys.* **108** 1089
[19] Pavlov A V 2011 *Geomag. Aeron.* **51** 143
[20] Huber H P and Herzberg G 1979 *Molecular Spectra and Molecular Structure IV Constants of Diatomic Molecules* (New York: Van Nostrand)
[21] Slanger T G and Cosby P C 1988 *J. Chem. Phys.* **92** 267
[22] Kajihara H, Okamura T and Koda S 1997 *J. Mol. Spectrosc.* **183** 72
[23] Edwards H G M, Good E A M and Long D A 1976 *J. Chem. Soc. Faraday Trans.* **72** 865
[24] Borrell P M, Borrell P and Ramsay D A 1986 *Can. J. Phys.* **64** 721
[25] Yoshino K, Murray J E, Esmond J R, Sun Y, Parkinson W H, Thoren A P, Learner R C M and Cox G 1994 *Can. J. Phys.* **72** 1101
[26] Wildt J, Bednarek G and Fink E H 1991 *Chem. Phys.* **156** 497
[27] Jenouvrier A, Mérienne M F, Coquart B, Carleer M, Fally S, Vandaele A C, Hermans C and Colin R 1999 *J. Mol. Spectrosc.* **198** 136
[28] García Muñoz A, Mills F P, Slanger T G, Piccioni G and Drossart P 2009 *J. Geophys. Res.* **114** E1202
[29] Ciping C and Ramsay D A 1993 *J. Mol. Spectrosc.* **160** 512
[30] Creek D M and Nicholls R W 1975 *Proc. B. Soc. Lond. A* **314** 517
[31] Schaefer H F and Harris F E 1968 *J. Chem. Phys.* **48** 4946
[32] Welch W M and Mizushima M 1972 *Phys. Rev. A* **5** 2692
[33] Saxon R P and Liu B 1977 *J. Chem. Phys.* **67** 5432
[34] Saxon R P and Liu B 1980 *J. Chem. Phys.* **73** 870
[35] Partridge H, Bauschlicher C W, Langhoff S R and Taylor P R 1991 *J. Chem. Phys.* **95** 8292

[36] Cosby P C and Huestis D L 1992 *J. Chem. Phys.* **97** 6108
[37] Luque R G, Merchán M, Fülscher M P and Roos B O 1993 *Chem. Phys. Lett.* **204** 323
[38] Yeager D L, Nichols J A and Golab J T 1994 *J. Chem. Phys.* **100** 6514
[39] Byrman C P and Lenthe J H V 1996 *Int. J. Quantum Chem.* **58** 351
[40] Beebe N H F, Thulstrip E K and Andersen A 1976 *J. Chem. Phys.* **64** 2080
[41] Minaev B F 2000 *Chem. Phys.* **252** 25
[42] Minaev B F and Minaeva V A 2001 *Phys. Chem. Chem. Phys.* **3** 720
[43] Minaev B F and Telyatnik L G 2001 *Opt. Spectrosc.* **91** 883
[44] Müller T, Dallos M, Dubrovay H L, Dubrovay Z and Szalay P 2001 *Theor. Chem. Acc.* **105** 227
[45] Jiang W Y and Wilson A K 2011 *J. Chem. Phys.* **134** 034101
[46] Werner H J, Knowles P J, Knizia G *et al.* 2010 MOLPRO: *a Package of ab initio Programs*
[47] Dunning T H 1989 *J. Chem. Phys.* **90** 1007
[48] Le Roy R J 2002 *LEVEL* 7.5*: a Computer Program for Solving the Radial Schrödinger Equation for Bound and Quasibound Levels* (University of Waterloo, Chemical Physics Research Report CP-655)
[49] Moore C E 1993 *Atomic energy levels* (Washington (DC): National Bureau of Standards)
[50] Bernath P 1996 *Phys. Today* **49** 94
[51] Shi Y B, Stancil P C and Wang J G 2013 *Astron. & Astraphys.* **551** A140
[52] Gredel R, Carpentier Y, Rouillé G, Steglich M, Huisken F and Henning Th 2011 *Astron. & Astraphys.* **530** A26